

## Non-Gaussian Distribution of Coulomb Blockade Peak Heights in Quantum Dots

A. M. Chang,<sup>1</sup> H. U. Baranger,<sup>1</sup> L. N. Pfeiffer,<sup>1</sup> K. W. West,<sup>1</sup> and T. Y. Chang<sup>2</sup>  
<sup>1</sup>AT&T Bell Laboratories, 600 Mountain Avenue, Murray Hill, New Jersey 07974-0636  
<sup>2</sup>AT&T Bell Laboratories, Crawfords Corner Road, Holmdel, New Jersey 07733  
 (Received 26 July 1995)

We have observed a strongly non-Gaussian distribution of Coulomb blockade conductance peak heights for tunneling through quantum dots. At zero magnetic field, a low-conductance spike dominates the distribution; the distribution at nonzero field is distinctly different and still non-Gaussian. The observed distributions are consistent with theoretical predictions based on single-level tunneling and the concept of “quantum chaos” in a closed system weakly coupled to leads.

PACS numbers: 72.20.My, 05.45.+b, 73.20.Dx, 73.23.Hk

Experimental mesoscopic physics has concentrated on transport through *open* systems, systems in which the conductance is larger than  $2e^2/h$  [1]. Mesoscopic effects in isolated systems or the localized regime have been extensively investigated theoretically [1] but have received only occasional experimental attention because of the difficulty of such experiments [2,3].

On the other hand, experiments addressing “quantum chaos” have traditionally concentrated on the distribution of eigenvalues in *closed* systems [4–7]. The statistical properties of the *wave functions*, however, have been more difficult to access. To date, only a few experiments have addressed this issue. These include the Porter-Thomas fluctuations in the resonance widths in elastic scattering from nuclei [8] and the recent work on spatial correlation of eigenmodes in microwave cavities [9,10].

The advent of GaAs/Al<sub>x</sub>Ga<sub>1-x</sub>As heterostructures and electron beam nanofabrication has opened up a readily accessible system for studying mesoscopic physics in *both* open and closed systems. Recent theoretical work has dealt specifically with the manifestations of quantum chaos in the mesoscopic transport properties of such systems [11–22]. While several experiments have addressed these manifestations in open systems [23–27], thus far signs of quantum chaos in the mesoscopic properties of closed systems have proved elusive (see [3], however).

In GaAs/Al<sub>x</sub>Ga<sub>1-x</sub>As devices, the closed system is implemented as a quantum dot weakly coupled to leads. The most striking experimental mesoscopic feature in quantum dots is the large fluctuation in the height of the conductance peaks in the Coulomb blockade regime [28,29]. This feature is more striking than the fluctuations in the peak spacing because the Coulomb energy is typically much larger than the level spacing. Inspired by these observations, Jalabert, Stone, and Alhassid predicted that in the limit of thermally broadened tunneling through a single quantum level, the conductance peak height,  $G_{\max}$ , should be statistically distributed with a strong enhancement near zero [18].  $G_{\max}$  fluctuates because the coupling to the leads depends on the magnitude of the level’s wave function near the leads, which fluctuates in both mesoscopic and quantum-chaotic systems [1,4]. In addition to the fluctua-

tions caused by single-particle effects included explicitly in the theory, there may be many-body contributions in the actual dots, but this is not expected to change qualitatively the statistical distribution. Subsequent work [19–22] extended the theory in several directions.

More precisely, when  $\Gamma \ll kT < \Delta$ , where  $\Gamma$  is the resonance width and  $\Delta$  the level spacing,  $G_{\max}$  for tunneling through a single nondegenerate level is [30]

$$G_{\max} = \frac{e^2}{h} \frac{\pi}{2kT} \frac{\Gamma_L \Gamma_R}{\Gamma_L + \Gamma_R} \equiv \frac{e^2}{h} \frac{\pi \bar{\Gamma}}{2kT} \alpha, \quad (1)$$

where  $\Gamma_L$  ( $\Gamma_R$ ) is the partial decay width into the left (right) lead. For  $B = 0$ , the predicted distribution is [18]

$$P_{(B=0)} = \sqrt{2/\pi\alpha} e^{-2\alpha}; \quad (2)$$

note the square-root singularity near zero. In a magnetic field greater than the correlation field, the breaking of time-reversal symmetry reduces the number of nearly zero values of  $G_{\max}$ . Nevertheless, the distribution [18,19] is still non-Gaussian and peaked near zero,

$$P_{(B \neq 0)} = 4\alpha [K_0(2\alpha) + K_1(2\alpha)] e^{-2\alpha}, \quad (3)$$

where  $K_n$  are the modified Bessel functions. In contrast, when many levels are involved in the tunneling, such as in a typical metallic dot of size 500 Å, the distribution should tend towards a Gaussian. While previous experiments have observed fluctuations in the peak height [28,29], these fluctuations are smaller than those predicted theoretically and, in particular, the predominance of very small peaks is not observed.

In this Letter, we report our observation of a *strongly non-Gaussian distribution* of Coulomb blockade conductance peak heights for tunneling through individual GaAs/Al<sub>x</sub>Ga<sub>1-x</sub>As quantum dots. This is the first systematic study of fluctuations in transport through a nearly isolated system. We find a strong enhancement of small values of  $G_{\max}$  in zero magnetic field, and a significant change in the distribution when a magnetic field is applied. The experimental distributions are consistent with the theoretical predictions above, which suggests that we are observing single-level tunneling.

Our devices are fabricated on a GaAs/Al<sub>x</sub>Ga<sub>1-x</sub>As heterostructure crystal with an electron density of  $1.7 \times$

$10^{11} \text{ cm}^{-2}$  and a transport mean free path of  $\sim 0.4 \mu\text{m}$ . As shown in Fig. 1, each quantum dot is defined via a pair of left pincher gates (narrow lines  $\sim 0.06 \mu\text{m}$  wide), a pair of right pincher gates, and a pair of central gates which controls the number of electrons on the dot (wider lines  $\sim 0.15 \mu\text{m}$ ). Four individual dots are available on each sample. Because of the presence of oval defects and trap states, not all dots are stable. To maximize the number of dots available, each pair of gates is tied together. Out of two samples studied, four individual dots were used.

The lithographic dimension of a dot is  $0.3 \mu\text{m} \times 0.35 \mu\text{m}$ . At typical gating voltages, depletion of electrons surrounding the gates reduces the effective size to  $\sim 0.25 \mu\text{m} \times 0.25 \mu\text{m}$ , yielding roughly 100 electrons on a dot. The short mean free path, only slightly larger than the dot, and the lithographic imperfections ensure that each dot is different and distorted from a true rectangle; thus the dynamics in the dot are certainly chaotic rather than regular. Interactions between electrons on the dot may cause additional chaos. On the other hand, the dot is clearly not in the diffusive regime customary for mesoscopic physics: momentum relaxation is caused predominantly by scattering from the smooth boundaries.

The typical capacitance of a dot to the surrounding gates is  $\sim 130 \text{ aF}$ , yielding a Coulomb charging energy of  $1.2 \text{ meV}$ . The mean level spacing is given by the Fermi energy ( $5.0 \text{ meV}$ ) divided by the number of electrons, giving roughly  $50 \mu\text{eV}$  ( $620 \text{ mK}$ ). Previous studies of the

peak height,  $G_{\text{max}}$ , as a function of electron temperature (deduced from the width of the resonance peak) indicate, however, that in order for nearly all peaks to be in the single-level regime, the electron temperature should be below  $200 \text{ mK}$  [28,29]. With RF filtering and electrical feedthroughs the lowest temperature achieved here is  $75 \text{ mK}$ . The measurements are performed using standard lock-in techniques at an excitation voltage of  $2.8 \mu\text{V rms}$ .

In Fig. 2 we show a representative trace of Coulomb blockade conductance peaks at  $B = 0$  and  $T = 75 \text{ mK}$ . Note first the missing peaks at the gate voltages  $-733$ ,  $-753$ , and  $-762 \text{ mV}$ . We are certain that peaks occur at these positions by observing them at either higher temperature or nonzero magnetic field. *The large difference in height of neighboring peaks and the many tiny peaks at small  $T$  are our primary experimental observation.* Second, note the variation in peak spacing in Fig. 2. Because of the changing occupancy of traps near the dot, the position of a peak switches between several gate voltages, typically within  $1 \text{ mV}$  compared to a spacing of  $\sim 6 \text{ mV}$ . In most cases ( $>90\%$ ), the change in position does not affect  $G_{\text{max}}$  by more than  $10\%$ , indicating that the traps contribute only an offset to  $V_g$ . The third feature is the decrease in overall conductance with increasingly negative  $V_g$ . This indicates that the left and right pinchers are closing, reducing the partial widths  $\Gamma_L$  and  $\Gamma_R$  which are determined by both the pincher transmission probabilities and the wave function near the pinchers.

In Fig. 3 we show magnetic field traces of  $G_{\text{max}}$  for four representative peaks. From the fastest variation of  $G_{\text{max}}$ , we estimate a correlation field,  $B_c$ , of the order of  $500 \text{ G}$ . This is somewhat larger than the theoretical value [18,20],  $B_c \sim 200 \text{ G}$ . Panels (c) and (d) show the behavior of two peaks which are nearly zero at  $B = 0$ . Even at the highest magnetic field of  $7.5 \text{ kG}$ , no regularity is observed in the peak heights associated with the formation

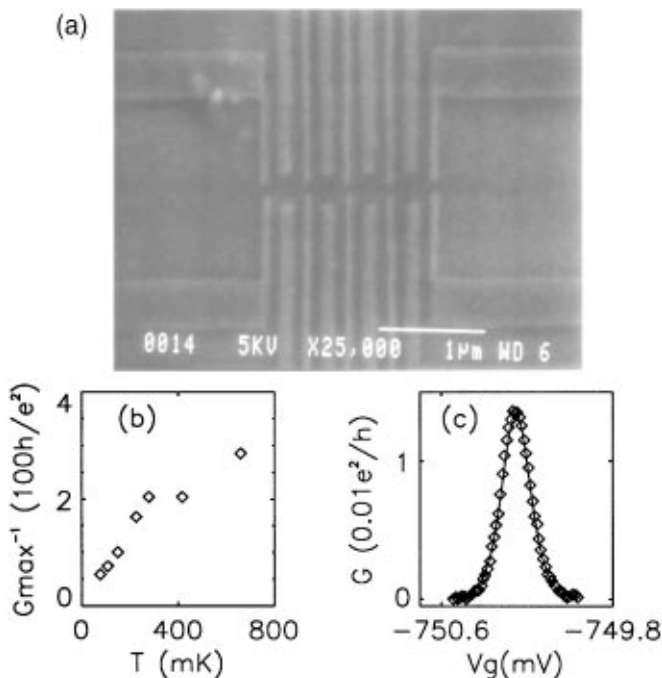


FIG. 1. (a) Electron micrograph of the gates defining the quantum dots. Four dots are available on each sample. (b)  $G_{\text{max}}^{-1}$  vs  $T$  for a representative peak at  $B = 0$ . The roughly linear behavior below  $\sim 300 \text{ mK}$  indicates this is a single-level tunneling peak. (c) A fit of the convolution of  $-\partial f/\partial \epsilon$  with the Breit-Wigner resonant tunneling formula to the peak in (b) at  $T = 108 \text{ mK}$ .

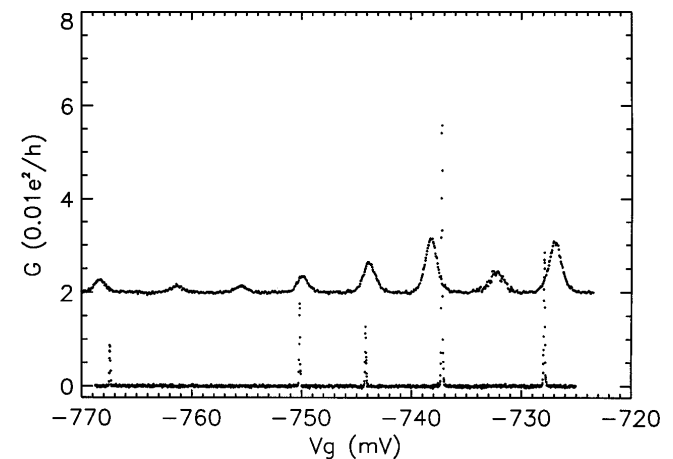


FIG. 2. A typical trace showing successive Coulomb blockade conductance peaks versus the center gate voltage,  $V_g$ .  $B = 0$  and  $T = 75 \text{ mK}$  (lower trace) or  $T = 660 \text{ mK}$  (upper trace, displaced by 2 units). Note that three peaks are missing out of seven, but they emerge at higher temperature. The slight shifting in peak positions is discussed in the text.

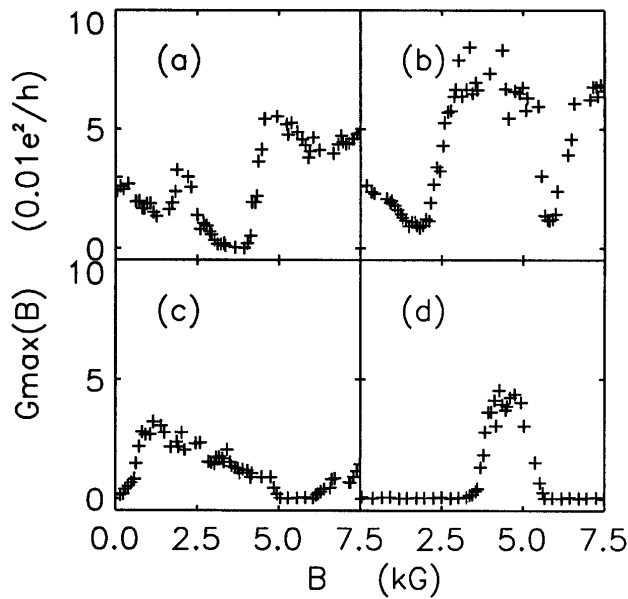


FIG. 3. Magnetic field sweep of four peaks at  $T = 100$  mK. The field range for  $\sim 100\%$  change in  $G_{\max}$  is  $\sim 500$  G. (c),(d) Two types of behavior of peaks which are very small at  $B = 0$ .

of Landau levels. This results from the inherent disorder and the small size of our dot  $\sim 0.25 \mu\text{m}$  compared to the cyclotron radius;  $\sim 0.2 \mu\text{m}$  wide quantum wires made from comparable crystals show no quantum Hall effect below 15 kG at  $T \approx 50$  mK [31].

Because of the variation of pincher transmission with  $V_g$ , we must select a subset of the observed peaks for the purpose of investigating the distribution of peak heights. Two physical criteria guide this selection: (1) the pincher transmission should not be too high because we want  $\Gamma < kT$ , and (2) it should not be too low, otherwise all peaks will be small simply because the transmission of the pinchers is small. A peak is accepted if  $G(V_g, B)$  attains a maximum value which satisfies  $(0.1e^2/h)/3.5 \leq \max_{[V_g, B]} G \leq 0.1e^2/h$ . The upper cutoff is chosen to ensure that all peaks satisfy criterion (1) above. The lower cutoff is chosen as a compromise to eliminate a bias toward small peaks caused by small pincher transmission while allowing the inclusion of a reasonable number of peaks. The fact the peak height attains a value greater than  $(0.1e^2/h)/3.5$  when  $B$  is swept shows the pinchers are not closed: if the peak is small at some particular  $B$ , its smallness is caused by small wave-function coupling probability, not small pincher transmission.

If the distribution is very strongly spiked near zero height, the variation in pincher transmission that we allow will not obscure the zero height enhancement or the non-Gaussian nature; for the theoretical distributions Eqs. (2) and (3), we have checked that there is little distortion upon averaging  $\bar{\Gamma}$  over a factor of 3.5 (see Fig. 4). Typically, the left and right pincher transmission are roughly equal, and 5 peaks are accepted for a given setting. By changing the pincher so that both the  $V_g$  and  $B$  traces are uncorre-

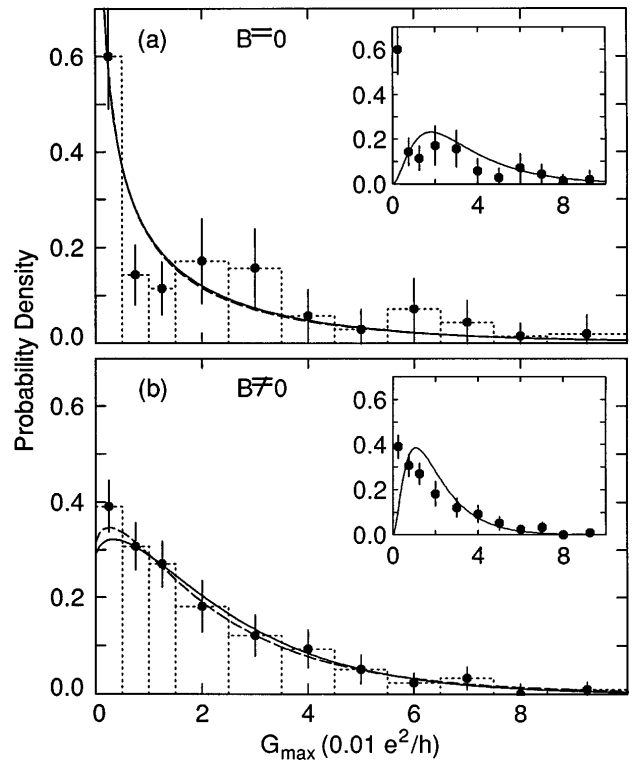


FIG. 4. Histograms of conductance peak heights for (a)  $B = 0$  and (b)  $B \neq 0$ . Data are scaled to unit area; there are 72 peaks for  $B = 0$  and 216 peaks for  $B \neq 0$ ; the statistical error bars are generated by bootstrap resampling. Note the non-Gaussian shape of both distributions and the strong spike near zero in the  $B = 0$  distribution. Fits to the data using both the fixed pincher theory (solid) and the theory averaged over pincher variation (dashed) are excellent. The insets show fits by  $\chi^2(\alpha)$ —a more Gaussian distribution—averaged over the pincher variation; the fit is extremely poor.

lated, we generate  $\sim 18$  peaks per dot; usually 10 mV out of  $\sim -500$  mV suffices, referenced to an electron gas depletion threshold of  $-280$  mV. In this manner, we gather 72 peaks for each value of  $B$ . Each peak is tracked as a function of magnetic field from 0 to 7.5 kG; data at  $B = 2.5, 5,$  and  $7.5$  kG are used for  $B \neq 0$  (note these values are separated by several  $B_c$ ).

In Fig. 4, we plot histograms of the observed peak heights for  $B = 0$  and  $B \neq 0$ . They are normalized to unit area as for a probability density; the bin size is smallest near 0 and is 3 times as large for the largest  $G_{\max}$ . *Both distributions are strongly non-Gaussian, and clearly peaked toward zero values.* In the  $B = 0$  case, nearly  $1/3$  of the peaks fall in the lowest bin: 23 out of 72 peaks are less than  $0.005e^2/h$  compared to a mean of  $\sim 0.024e^2/h$ . In contrast, for  $B \neq 0$  only 43 out of 216 peaks are this small. Figure 4 indicates that there is a difference between the two distributions for low values, but the statistical fluctuations obscure any difference for large values. This indication is confirmed by statistical analysis: using standard methods (the Kolmogorov-Smirnov test and testing whether the difference distribution is consistent with zero [32]), we find that the two distributions are significantly

different for  $G_{\max} \leq 0.02e^2/h$  (significance  $\leq 0.03$ ) while being only modestly different overall (significance  $\approx 0.1$ ).

Finally, we compare the experimental distributions to the theoretical predictions Eqs. (2) and (3). To make this comparison legitimately, one should be in the regime  $\Gamma \ll kT \ll \Delta$ ; we believe that this is largely the case. First, for a tunneling peak in this limit  $G_{\max}^{-1}(T)$  should be linear; see Eq. (1). In Fig. 1(b) we plot  $G_{\max}^{-1}$  versus  $T$  for a typical peak, showing the linear behavior. In fact, all eight peaks for which we have detailed temperature dependence and dynamic range above noise ( $G_{\max} \geq 0.005e^2/h$ ) show linear behavior. For nearly zero height peaks ( $G_{\max} \leq 0.005e^2/h$ ), although we cannot directly demonstrate that  $G_{\max}^{-1}(T)$  is linear, the measured  $G_{\max}$  is an upper bound: if neighboring thermally accessible levels were highly conducting, the observed height would be enhanced above that of the low-conductance single level alone. Thus we have underestimated the zero height enhancement in our data set. Figure 1(c) shows a fit of the line shape at  $T = 108$  mK by the functional form  $G \propto \cosh^{-2}[(E_0 - \alpha eV_g)/2kT]$  appropriate for tunneling through a thermally broadened level ( $\Gamma \ll kT$ ) [30]. Since  $G_{\max}$  is constrained below  $0.1e^2/h$ , assuming roughly equal  $\Gamma_L$  and  $\Gamma_R$ , we have  $\Gamma \leq kT/5\pi$ .

The mean decay width needed for comparing to the theory is not measured experimentally and is therefore a fitting parameter. This width should not depend on  $B$ , however, so we introduce a single scale parameter and fit simultaneously to the  $B = 0$  and  $B \neq 0$  data. Figure 4 shows a fit to the data using both the theory for constant pincher transmission [Eqs. (2) and (3) (solid)] and this theory averaged over a variation of the pincher transmission by a factor of 3.5 (dashed). The similarity of the two curves shows that the variation in our pincher transmission can be neglected. The “goodness of fit,” denoted  $f$ , for the solid line in Fig. 4 is 0.65 (the probability that the deviation from the model could be caused by statistical fluctuations [32]). In contrast, in the insets we show the best fit of the data with a  $\chi^2$  distribution with 6 degrees of freedom averaged over the pincher variation. This distribution is closer to a Gaussian and clearly does not describe the data ( $f < 10^{-4}$ ). In addition, the data for  $B = 0$  are strongly inconsistent with the  $B \neq 0$  theory.

We conclude that (1) we have observed a distribution of conductance peak heights with a large zero height enhancement, (2) the distribution changes as the magnetic field breaks time-reversal symmetry, and (3) our data are consistent with the single-level tunneling theory.

- 
- [1] For reviews see C. W. J. Beenakker and H. van Houten, in *Solid State Physics*, edited by H. Ehrenreich and D. Turnbull (Academic Press, New York, 1991), Vol. 44; B. L. Altshuler, P. A. Lee, and R. A. Webb, *Mesoscopic Phenomena in Solids* (North-Holland, Amsterdam, 1991).  
 [2] Representative experiments include L. P. Lévy *et al.*, Phys. Rev. Lett. **64**, 2074 (1990); V. Chandrasekar *et al.*, Phys.

- Rev. Lett. **67**, 3578 (1991).  
 [3] L. P. Lévy, D. H. Reich, L. N. Pfeiffer, and K. W. West, Physica (Amsterdam) **189B**, 204 (1993).  
 [4] For a review see M. C. Gutzwiller, *Chaos in Classical and Quantum Mechanics* (Springer-Verlag, New York, 1990).  
 [5] H.-J. Stockmann and J. Stein, Phys. Rev. Lett. **64**, 2215 (1990).  
 [6] H.-D. Gräf, H. L. Harney, H. Lengeler, C. H. Lewenkopf, C. Rangacharyulu, A. Richter, P. Schardt, and H. A. Weidenmüller, Phys. Rev. Lett. **69**, 1296 (1992).  
 [7] A. Kudrolli, S. Sridhar, A. Pandey, and R. Ramaswamy, Phys. Rev. E **49**, R11 (1994).  
 [8] C. E. Porter and R. G. Thomas, Phys. Rev. **104**, 483 (1956).  
 [9] S. Sridhar, Phys. Rev. Lett. **67**, 785 (1991); A. Kudrolli *et al.*, Phys. Rev. Lett. **75**, 822 (1995).  
 [10] J. Stein and H.-J. Stockmann, Phys. Rev. Lett. **68**, 2867 (1992); J. Stein *et al.*, Phys. Rev. Lett. **75**, 53 (1995).  
 [11] R. A. Jalabert, H. U. Baranger, and A. D. Stone, Phys. Rev. Lett. **65**, 2442 (1990).  
 [12] H. U. Baranger, R. A. Jalabert, and A. D. Stone, Phys. Rev. Lett. **70**, 3876 (1993); Chaos **3**, 665 (1993).  
 [13] W. A. Lin, J. B. Delos, and R. V. Jensen, Chaos **3**, 655 (1993); R. V. Jensen, Chaos **1**, 101 (1991).  
 [14] H. U. Baranger and P. A. Mello, Phys. Rev. Lett. **73**, 142 (1994); Phys. Rev. B **51**, 4703 (1995).  
 [15] R. A. Jalabert, J.-L. Pichard, and C. W. J. Beenakker, Europhys. Lett. **27**, 255 (1994).  
 [16] Z. Pluhar, H. A. Weidenmüller, J. A. Zuk, and C. H. Lewenkopf, Phys. Rev. Lett. **73**, 2115 (1994).  
 [17] K. B. Efetov, Phys. Rev. Lett. **74**, 2299 (1995).  
 [18] R. A. Jalabert, A. D. Stone, and Y. Alhassid, Phys. Rev. Lett. **68**, 3468 (1992).  
 [19] V. N. Prigodin, K. B. Efetov, and S. Iida, Phys. Rev. Lett. **71**, 1230 (1993); Phys. Rev. B **51**, 17223 (1995).  
 [20] H. Bruus and A. D. Stone, Phys. Rev. B **50**, 18275 (1994).  
 [21] E. R. Mucciolo, V. N. Prigodin, and B. L. Altshuler, Phys. Rev. B **51**, 1714 (1995).  
 [22] Y. Alhassid and C. H. Lewenkopf (to be published).  
 [23] C. M. Marcus, A. J. Rimberg, R. M. Westervelt, P. F. Hopkins, and A. C. Gossard, Phys. Rev. Lett. **69**, 506 (1992); I. H. Chan *et al.*, Phys. Rev. Lett. **74**, 3876 (1995).  
 [24] M. W. Keller, O. Millo, A. Mittal, D. E. Prober, and R. N. Sacks, Surf. Sci. **305**, 501 (1994).  
 [25] A. M. Chang, H. U. Baranger, L. N. Pfeiffer, and K. W. West, Phys. Rev. Lett. **73**, 2111 (1994).  
 [26] M. J. Berry, J. A. Katine, R. M. Westervelt, and A. C. Gossard, Phys. Rev. B **50**, 17721 (1994).  
 [27] J. P. Bird, K. Ishibashi, Y. Aoyagi, T. Sugano, and Y. Ochiai, Phys. Rev. B **50**, 18678 (1994).  
 [28] J. H. F. Scott-Thomas, S. B. Field, M. A. Kastner, D. A. Antoniadis, and H. I. Smith, Phys. Rev. Lett. **62**, 583 (1989); U. Meirav *et al.*, Phys. Rev. Lett. **65**, 771 (1990).  
 [29] E. B. Foxman, U. Meirav, P. L. McEuen, M. A. Kastner, O. Klein, P. A. Belk, D. M. Abusch, and S. J. Wind, Phys. Rev. B **50**, 14193 (1994).  
 [30] C. W. J. Beenakker, Phys. Rev. B **44**, 1646 (1991).  
 [31] A. M. Chang *et al.*, Solid State Commun. **67**, 769 (1988).  
 [32] W. H. Press, B. P. Flannery, S. A. Teukolsky, and W. T. Vetterling, *Numerical Recipes* (Cambridge University Press, New York, 1990).